For submission to MPE

Mitochondrial phylogenomics and genome rearrangements in the barklice (Insecta: Psocodea)

Kazunori Yoshizawa [a*], Kevin P. Johnson [b], Andrew D. Sweet [b], Izumi Yao [a], Rodrigo L. Ferreira [c], Stephen L. Cameron [d]

a Systematic Entomology, School of Agriculture, Hokkaido University, Sapporo 060-8589, Japan

b Illinois Natural History Survey, University of Illinois, Champaign, IL 61820, USA

c Biology Department, Federal University of Lavras, 37200-000 Lavras, MG, Brazil

d Department of Entomology, Purdue University, West Lafayette, IN 47907, USA

*corresponding author. Tel: +81-11-706-2424. E-mail: psocid@res.agr.hokudai.ac.jp

ABSTRACT

The mitochondrial genome arrangement in the insect order Psocodea (booklice, barklice, and parasitic lice) is extremely variable. Genome organization ranges from the rearrangement of a few tRNAs and protein coding genes, through extensive tRNA and protein coding gene rearrangements, to subdivision into multiple mini-chromosomes. Evolution of the extremely modified mitochondrial genome in parasitic lice (Phthiraptera) has been the subject of several studies, but limited information is available regarding the mitochondrial genome organization of the more plesiomorphic, free-living Psocodea (formerly known as the "Psocoptera"). In particular, the ancestral state of the psocodean mitochondrial genome arrangement and the evolutionary pathway to the rearranged conditions are still unknown. In this study, we addressed mitochondrial evolutionary questions within the Psocodea by using mitochondrial genome sequences obtained from a wide range of Psocoptera, covering all three suborders. We identified seven types of mitochondrial genome arrangements in Psocoptera, including the first example in Psocodea of retention of the ancestral pancrustacean condition in *Prionoglaris* (Prionoglarididae). Two methods (condition-based parsimony reconstruction and common-interval genome distances) were applied to estimate the ancestral mitochondrial arrangement in Psocodea, and both provided concordant results. Specifically, the common ancestor of Psocodea retained the ancestral pancrustacean condition, and most of the gene arrangement types have originated independently from this ancestral condition. We also utilized the genomic data for phylogenetic estimation. The tree estimated from the mitochondrial genomic data was well resolved, strongly supported, and in agreement with previously estimated phylogenies. It also provided the first robust support for the family Prionoglarididae, as its monophyly was uncertain in previous morphological and molecular studies.

Keywords: mitochondrial genome, gene rearrangements, Psocodea, Psocoptera, Prionoglarididae, phylogeny

1. Introduction

During the last couple of decades, sequences of the mitochondrial genome from hundreds of insect species have been obtained. These sequences have been used for phylogenetic analyses at both deep and shallow levels, as well as for analyses of mitochondrial genome organization (Cameron, 2014a, 2014b). As the sequences of more and more insect mitochondrial genomes have been obtained, it has become clear that, although gene arrangement is quite stable throughout many insects (the ancestral Pancrustacean condition is by far the most common mitochondrial genome arrangement observed), rearrangements of a few transfer RNA genes (tRNAs) are also quite common (Cameron, 2014a). In contrast, more extensive gene rearrangements, particularly those involving protein-coding genes (PCGs) or ribosomal RNA genes (rRNAs), are rather rare events and are common in only a few insect orders (Embioptera: Kômoto et al., 2012; Thysanoptera: Shao and Barker, 2003; Psocodea: Shao et al., 2001a; Hymenoptera: Mao et al., 2015). Extensive gene rearrangements, however, also occur in a number of highly derived members of orders in which most other taxa lack major rearrangements (e.g. Cecidomyiidae, Diptera: Beckenbach, 2012; Iberobaeniidae, Coleoptera: Andujar, 2017; Enicocephalidae, Hemiptera: Li et al., 2012; Aleyrodidae, Hemiptera: Thao et al. 2004).

Among insects, the highest variation in mitochondrial gene arrangement occurs in the order Psocodea (booklice, barklice, and parasitic lice, formerly known as two independent orders, "Psocoptera" and Phthiraptera: Yoshizawa and Johnson, 2006). The mitochondrial variation observed in Psocodea ranges from the rearrangement of a few tRNAs and two PCGs in the suborder Psocomorpha (Shao et al., 2001b; Cameron, 2014a; Li et al., 2013), through extensive tRNA and PCG rearrangements in the suborder Trogiomorpha (Shao et al., 2003), the family Liposcelididae (Shi et al., 2016), and Phthiraptera (e.g., Shao et al., 2001a), to extreme subdivision into multiple mini-chromosomes in some Liposcelididae (Chen et al., 2014) and Phthiraptera (Shao et al., 2009, 2015; Cameron et al., 2011). Evolution of the extremely modified mitochondrial genome in Phthiraptera has been the subject of several studies (e.g., Shao et al., 2001a, 2009, 2015; Cameron et al., 2011). However, other than the family Liposcelididae (the sister-group of the parasitic lice, with many reduced traits

similar to parasitic lice; Yoshizawa and Lienhard, 2010), limited information is available for the more plesiomorphic, free-living Psocodea (formerly the "Psocoptera"). Therefore, the ancestral condition of the psocodean mitochondrial genome arrangement is still unknown. In addition, extensive mitochondrial rearrangements are also known from thrips (Thysanoptera) (Shao and Barker, 2003; Yan et al., 2014; Dickey et al., 2015; Liu et al., 2017), an order classified with Psocodea as part of the superorder Paraneoptera (Yoshizawa and Lienhard, 2016). Additional mitochondrial genomic information from free-living Psocodea is thus crucial to inferring both the ancestral mitochondrial genome organization of Psocodea and for understanding supra-ordinal level evolution of the mitochondrial genome.

Additional mitochondrial genome data from Psocodea will also contribute to our phylogenetic understanding of the order. Although the higher-level phylogenetic relationships within Psocodea have been the subject of several studies (e.g., Yoshizawa et al., 2006; Yoshizawa and Johnson, 2010, 2014), unresolved problems still remain. One of these concerns the monophyly of the Prionoglarididae (suborder Trogiomorpha). Because the family is known to retain many plesiomorphic features (Lienhard, 1998; Yoshizawa et al., 2006), its monophyly is highly controversial. Although one previous molecular phylogenetic analysis (Yoshizawa et al., 2006: fig. 2) provided support for the monophyly of Prionoglarididae, analyses with more extensive taxon or gene samplings (Yoshizawa et al., 2006: fig. 3; Yoshizawa and Johnson, 2014) suggested the family may be paraphyletic. As mentioned above, this family retains the most plesiomorphic morphology among the extant Psocodea, and so resolving the status of Prionoglarididae has great impact on how we interpret ancestral states and the evolution of the Psocodea.

In this study, we address both phylogenetic and mitochondrial evolutionary questions within the Psocodea by using the mitochondrial genome sequences obtained from a wide range of free-living Psocodea. The selected taxa cover all three suborders of the “Psocoptera”. In particular, three genera representing both subfamilies of the Prionoglarididae were sampled to test the monophyly of this family and also to examine the origin of the extensive gene rearrangements previously recorded in members of the suborder Trogiomorpha. Two methods of the ancestral state estimation, condition-based coding with parsimony reconstruction and common-

interval genome distances (implemented in the TreeREx software: Bernt et al., 2007, 2008), are compared to test the effectiveness of these methods for ancestral state reconstruction.

2. Materials and Methods

2.1. Samples

Ten species (Table 1) were sequenced representing all three of the free-living suborders of Psocodea, including eight different families. In addition, sequences of Lepidopsocidae sp. (Shao et al., 2003), *Stenocaecilius quercus* (= *Caecilius quercus*: Shao et al., 2001b), *Psococerastis albimaculata*, and *Longivalvus hyalospilus* (Li et al., 2013) were obtained from GenBank. Mitochondrial genomes have also been previously sequenced for parasitic lice (Phthiraptera) and booklice (Liposcelididae). However, sequences from both groups were excluded from the present study due to their extremely high rates of mitochondrial genome rearrangement and fragmentation (Cameron et al., 2011; Chen et al., 2014; Shao et al., 2017), which obscure genome evolution events within free-living Psocodea. Two outgroup sequences, *Abidama producta* (Cercopidae, Hemiptera: an order classified to Paraneoptera together with Psocodea) and *Dysmicohermes ingens* (Corydalidae, Megaloptera: an order of Holometabola, the sister taxon of Paraneoptera), were also obtained from GenBank.

2.2. Sequencing and assemblying

DNA was extracted using a Qiagen QIAamp DNA Micro Kit or DNeasy Blood and Tissue Kit. DNA of *Dorypteryx*, *Prionoglaris*, and *Neotrogla* was sheared using a Covaris M220 instrument to approximately 400 bp and sequence libraries were prepared using a Kapa Library Preparation kit. Libraries were pooled with two other taxa and sequenced together in a single lane with 160 bp paired-end reads on an Illumina HiSeq 2500. Raw reads are deposited in NCBI SRA (SRR5308267, SRR5308282, SRR5308278). To obtain mitochondrial genome sequences from these libraries we generated contigs using a combination of aTRAM (Allen et al., 2015) and MITObim (Hahn et al. 2013). First, aTRAM was used to assemble five protein-coding mitochondrial genes (*cox1*, *cox2*, *cob*, *nad2*, and *nad5*) for each genus using amino acid sequences as targets for these assemblies. In all cases, aTRAM

was run for a single iteration on 10% of the paired-end libraries, and contigs were assembled in aTRAM using ABySS (Simpson et al. 2009). Second, MITObim was used to extend the contigs assembled with aTRAM by using each contig as a starting reference for that species. Additionally, partial previously generated Sanger sequences of *rrnS* were used as starting references for all three genera, and Sanger sequences of *rrnL* as starting references for *Dorypteryx* and *Prionoglaris*. MITObim was then run for each starting reference a maximum of 100 iterations, using either 10% (*Dorypteryx* and *Prionoglaris*) or 20% (*Neotrogla*) fractions of the paired-end libraries. To obtain *trnI* and *trnM* sequences for *Neotrogla*, we used aTRAM with sequences of these tRNAs from the *Prionoglaris* and *Speleketor* genomes in this study. A small region not recovered by aTRAM and MITObim (part of *nad4* and *nad4l* of *Prionoglaris*) was amplified by PCR and sequenced by Beckman CEQ2000 Sanger sequencer (Yoshizawa & Johnson, 2003).

The complete mitochondrial genomes of *Speleketor*, *Stimulopalpus*, *Archipsocus*, *Lachesilla* and *Amphigerontia*, and partial mitochondrial genomes for *Echmepteryx* and *Trogium*, were amplified by long PCR and sequenced by primer walking (Cameron 2014b). Long PCRs were performed with Elongase (Invitrogen), Sanger sequenced with the ABI Big Dye ver3 chemistry and run on an ABI 3770 automated sequencer. Amplification primers are listed in Supplementary Table S1. Long PCR and sequencing conditions match those used in Cameron et al. (2011).

2.3. Annotations

The MITOS server (Bernt et al., 2013) was used for initial annotation. However, the MITOS server often could not correctly identify the start and stop codons, so these were manually annotated by aligning the sequences with the annotated mitochondrial genome data of the other Psocodea downloaded from GenBank (Cameron 2014b).

2.4. Alignment

Protein coding genes (PCGs) were aligned based on translated amino-acids using Muscle (Edgar, 2004) implemented in MEGA 7 (Kumar et al., 2016). Ribosomal RNAs (rRNA) were aligned using MAFFT 6.5 (Katoh and Standley, 2013) with the Q-

INS-i option, in which secondary structure information of RNA is considered. Apparent misalignments were corrected manually. Transfer RNAs (tRNAs) were manually aligned based on secondary structure models estimated in MITOS. Poorly aligned regions (such as hyper variable regions of RNAs near the start and stop codons of PCGs) were excluded from the analyses.

2.5. Data set

We prepared the following six data sets: (1) ALL = all protein coding and RNA genes; (2) ex.3rd = all protein coding genes (third codon position excluded) and RNA genes; (3) PCG = all protein coding genes; (4) PCG12 = all protein coding genes (third codon position excluded); (5) RNA = all RNA genes; (6) AA = amino-acid sequences of the PCG dataset. For each data set, two taxon sets were prepared: (1) all taxa and (2) excluding taxa with missing data (*Stenocaecilius*, *Echmepteryx*, and *Trogium*).

For detecting potential biases affecting the accuracy of phylogenetic estimation using mitochondrial genome data (Sheffield et al., 2009), AT content and P-distances were calculated by using MacClade 4 (Maddison and Maddison, 2000) and PAUP* 4.0a152 (Swofford, 2002), respectively. AT content was calculated for each PCG gene, combined tRNAs, each rRNA, and codon positions (PCG1, 2, 3). A chi-square test of base homogeneity was performed using PAUP*.

2.6. Model selection

The best substitution models and partition schemes for the maximum likelihood (ML) and Bayesian analyses were estimated using PartitonFinder 2.1.1 (Lanfear et al., 2017), with the greedy algorithm. Taxa with missing data were excluded for model estimation to avoid the potential negative effects caused by missing data. The following partitions were predefined for the PartitionFinder analyses: codon positions for each PCGs (13 genes x 3 codons = 39 partitions), tRNAs (22 partitions), and rRNAs (2 partitions)

2.7. Tree Search

We estimated a maximum likelihood tree using IQ-Tree 1.4.3 (Nguyen et al.,

2015), with 1000 replicates of ultrafast likelihood bootstrap (Minh et al., 2013) to obtain bootstrap branch support values. Bayesian analyses were performed using MrBayes (Ronquist and Huelsenbeck, 2003). We performed two runs each with four chains for 500 000 generations, and trees were sampled every 100 generations. The first 50% of sampled trees was excluded as burn-in, and a 50% majority consensus tree was computed to estimate posterior probabilities. To evaluate the potential impact of substitution rate and compositional biases on phylogeny estimation, we also performed tree searches using PhyloBayes 4.1 (Lartillot et al., 2009) under a heterogeneous (CAT+GTR) model. We ran two independent tree searches for 10,000 cycles. However, for the PCG12 data, the two runs did not converge by 10,000 cycles (maxdiff > 0.3), so we ran 20,000 cycles for this data set. The first 50% of sampled trees were excluded as burn-in, and trees were sampled every 10 cycles. A majority consensus tree was computed from the two combined runs.

2.8. Character Coding and Ancestral State Estimation

Each genome was compared to the inferred ancestral insect mitochondrial genome (present in both outgroup taxa) to examine pairs of adjacent genes or gene-boundaries. Novel gene boundaries, those not observed in the ancestral insect mitochondrial genome, were coded as binary characters (either present or absent). Genome rearrangements result in new gene-pairs from both the insertion of a gene/gene-block at a novel location and from its deletion from the ancestral location. Both of these types of events were coded separately (Fig. 1: insertions labelled with numbers, deletions labelled with letters). For example, in *Speleketor* the translocation of *trnC* results in both *trnC-trnQ*, a novel boundary formed by an insertion, whereas *trnW-trnY* is also a novel boundary but was formed by the deletion of *trnC* from its ancestral location, the *trnW-trnC-trnY* condition. This condition-based data matrix was optimized parsimoniously on the best phylogenomic tree obtained from the ALL dataset (see above) using MacClade.

We also reconstructed the gene rearrangement history by using TreeREx 1.85 (Bradt et al., 2008). TreeREx reconstructs genomic evolution based on common intervals (blocks of genes shared between taxa in a clade) and a defined phylogeny, allowing the inference of tandem-duplicate-random-loss events (TDRL after Boore,

2000), simple transpositions, inversions and inversion-transpositions (the latter three models can also be coded in the condition-based matrix described above). However, there are limitations to TreeREx, particularly that gene-duplications are not allowed, even though these are comparatively common in rearranged mitochondrial genomes and are an inferred mid-point in the TDRL model (after tandem duplication but prior to random loss). Duplicated genes were identified in two of the taxa sequenced in this study, two control regions (CR) are present in *Neotrogla* and *Speleketor*. Therefore, for these, only the CR at a novel position (indicated by asterisk in Fig. 1) was coded.

3. Results

3.1. Sequencing, Annotation, and Data Evaluation

Eight new, complete/nearly complete (missing only a portion of control region) mitochondrial genomes were sequenced representing five additional psocodean families and each of the three free-living suborders: Trogiomorpha (Prionoglarididae: *Prionoglaris stygia* 15,684+ bp at 67x mean coverage, *Neotrogla* sp. 16894+ bp at 81x mean coverage, *Speleketor irwini* 16,849bp at 66x mean coverage, Psyllipsocidae: *Dorypteryx domestica* 18,512+ bp at 320x mean coverage), Troctomorpha (Amphientomidae: *Stimulopalpus japonicus* 14,904bp) , and Psocomorpha (Archipsocidae: *Archipsocus nomas* 15,349bp, Lachesillidae: *Lachesilla anna* 16,236bp Psocidae: *Amphigerontia montivaga* 15,566+ bp). Additionally, partial mitochondrial genomes were sequenced for two additional families of Trogiomorpha, Trogiidae (*Trogium pulsatorium*) and Lepidopsocidae (*Echmepteryx hageni*), to confirm genome rearrangements previously reported in the latter family (Shao et al., 2003) (Supplementary Table S2).

These genomes were sequenced by a mix of methods including long-PCR followed by primer walking (Cameron, 2014b), direct NGS sequencing of extracted DNA (also known as genome skimming, Linard et al., 2015), and a combination of both methods. The control region (CR) of *Stimulopalpus* could not be amplified by long-PCR and a combination of PCR and NGS derived sequences allowed the sequences of genes flanking the CR to be determined for this species. The *trnI-trnM* genes of *Neotrogla* were assembled separately from the other mitochondrial genes using NGS approaches, and the two contigs could not be connected into a single

sequence. Therefore, the possibility that they are on separate mini-chromosomes or that they represent pseudogenes cannot be excluded. However, phylogenetic analyses of the *trnI* and *trnM* genes alone placed those from *Neotrogla* in the expected position, consistent with them being the functional copy of these genes in this species. In addition, homologous repeat units (38–42 or 66–73 bp/repeat, Supplementary Fig. S1) were identified at the 3' end of the *trnI-trnM* contig and the 5' end of the *trnQ…rrnS* contig. Therefore, it is very likely that these contigs are connected via this repeat region. No homologous sequence was detected between the 3' end of *rrnS* and the 5' end of *trnI*, except that both are AT rich. Repeat units of this size present known assembly problems for Illumina HiSeq reads, and it seems more likely that these regions failed to assemble rather than the two assembled contigs represent separate mini-chromosomes. Repeat units were also identified in the control regions of several other sequenced species including *Speleketor* (two repeat classes 20 x 30bp, 3 x 44bp respectively), *Stimulopalpus* (3x 108bp), *Lachesilla* (7x 121bp), and *Amphigerontia* (5x 149bp) (Supplementary Table S2), although none of these species failed to assemble into a single contig. Sequence level homology between repeat units in different taxa was not identified.

3.2. Genome Rearrangements

A total of seven genome arrangement types (1–6 and 6') were detected in free-living Psocodea, four of them (1–3, 5) for the first time (Fig. 1). Type 1, identified in *Prionoglaris* (Prionoglarididae) was identical to the ancestral Pancrustacean condition. Both *Neotrogla* (type 2) and *Speleketor* (type 3) possess unique tRNA rearrangements, but they share a novel rearrangement of *trnM* to between duplicated control regions. All species of non-prionoglarid trogiomorphs possess a complicated rearrangement involving 7 tRNAs and *cox2* (type 4), first identified in Lepidopsocidae (Shao et al., 2001ab), but now identified by our study as also occurring in Trogiidae and Psyllipsocidae. The rearranged tRNA block in non-prionoglarid trogiomorphs includes a novel boundary, *trnI-trnM* (Character 1: Fig. 1), that is also observed in *Neotrogla*. *Stimulopalpus* (type 5) also closely resembles the ancestral pancrustacean mitochondrial genome, with one tRNA inverted (*trnI*) and one tRNA transposed (*trnM/trnQ*). All species of Psocomorpha share a complicated

rearrangement of the genes *nad3*, *nad5*, and associated tRNAs (type 6). In addition, *Stenocaecilius* (type 6') likely has a secondary tRNA transposition (*trnE-trnS1*, character 17), but is otherwise the same as other psocomorphans. However, the tRNAs rearrangements between CR and *nad2* identified in other psocomorphans have not been sequenced for *Stenocaecilius*.

In addition to gene rearrangements, a couple of long non-coding regions were identified in *Neotrogla*: 97 bp between CR repeat units and *trnQ*, 96 bp between *trnQ* and *nad2*, and 255 bp between *nad4L* and *trnT*. The former two non-coding regions correspond to the prior positions of *trnI* and *trnM*, respectively, in the ancestral Pancrustacean mitochondrial genome, and may represent 'junk' DNA regions left over from the rearrangement event which resulted in the transposition of these genes. Evidence for this interpretation lies in the identification of a characteristic hair-pin structure similar to the anticodon arm of *trnI* within the 97 bp non-coding region between CR repeats and *trnQ* (Supplementary Fig. S2).

3.3. Mito-phylogenomics (Fig. 2)

The aligned DNA data matrix consisted of 15 360 bp in total length (11 436 bp for PCG and 3 294 for RNA: Supplementary Data S1), of which 1 077 bp of PCG and 684 bp of RNA data were excluded from the analyses because of highly unreliable alignment. Within the PCG data (after excluding unaligned sites), 7 023 sites were variable, of which 1 281 sites were phylogenetically informative. Within the RNA data, 1 545 sites were variable, of which 467 sites were phylogenetically informative. Within the aligned AA data, 2 261 of 3 453 total sites were variable, of which 510 sites were phylogenetically informative.

Plots of P-distance showed that homoplasies caused by multiple substitutions were not problematic for phylogenetic estimation, except for the 3rd codon position where the slope of plots seemed to plateau (Supplementary Fig. S3). Although significant codon heterogeneity was detected by chi-square test in all data sets ($p = 0.000$), comparisons of base composition suggested that there seemed no directional base composition biases causing artificial phylogenetic affinities (Fig. 2; Supplementary Table 3). Comparing datasets including versus excluding third codon positions and RNA genes, and using multiple inference methods, allowed us to

334 further test if these factors resulted in artefactual relationships or nodal support.
335 Trees estimated from six data sets, each with two taxon sets
336 (including/excluding taxa with missing data), were all concordant. Only one exception
337 was the placement of *Stenocaecilius* (the taxon with a large amount of missing data:
338 Fig. 1): it was placed as sister to *Lachesilla* with high support values in almost all
339 datasets, but was placed at the base of Psocomorpha by RNA data with very low
340 support values (<50% bootstrap [BS] and posterior probability [PP]). *Stenocaecilius*
341 lacked large amounts of data, including two rRNAs that occupied the largest
342 proportion of the RNA dataset. Although support values for the placement of taxa with
343 missing data were relatively low (66–97% BS and 77–100% PP: *Echmepteryx,*
344 *Trogium*, and *Stenocaecilius* [except for the placement by RNA dataset discussed
345 above]), almost all other branches were supported with very high support values
346 (>99% BP and 100% PP). Therefore, there were almost no detectable differences
347 caused by different data/taxon sets and analytical methods. The only exception
348 concerned the monophyly of Prionoglarididae: the family was consistently recovered
349 as a monophyletic group (Fig. 2), but its support values were significantly lower than
350 other branches (Table 2), although there were no missing data in three prionoglaridid
351 taxa. The support values were high in combined PCG+RNA or in separated RNA
352 analyses (over 80% BS and 100% PP) (Table 2). In contrast, when the PCG and
353 amino-acid data were analyzed separately, monophyly of Prionoglarididae generally
354 received lower support values (Table 2). Increasing the size of the data set generally
355 increased support for this clade, as was evident by comparing the results from RNA
356 or PCG to All. Exclusion of the highly homoplasious 3rd codon position did not
357 change the results significantly (ex.3rd and PCG12 datasets: Table 2).
358 Monophyly of the suborder Trogiomorpha was robustly supported. The
359 trogiomorphs excluding Prionoglarididae formed a clade (*Echmepteryx–Dorypteryx*
360 clade), in which *Dorypteryx* placed to the sister of the rest (= infraorder Atropetae).
361 The support values for the relationships among taxa within this clade were relatively
362 low, most probably due to large amount of missing data in *Trogium* and *Echmepteryx*.
363 *Stimulopalpus* was placed sister to Psocomorpha with high support values.
364 *Stimulopalpus* was the only representative sampled here from the suborder
365 Troctomorpha, so the monophyly of this suborder could not be tested. Monophyly of

366 the suborder Psocomorpha was robustly supported, with *Archipsocus*
367 (Archipsocetae: Archipsocidae) sister to the rest of psocomorphans with high support
368 values. *Stenocaecilius* (Caeciliusetae: Caeciliusidae) and *Lachesilla*
369 (Homilopsocidea: Lachesillidae) formed a clade with high support values. The
370 remaining three samples all belong to the Psocidae, and its monophyly was robust.
371
372 *3.4. Estimation of the History of Rearrangements*
373 A total of 28 characters (17 insertion and 11 deletion characters) were coded
374 (Supplementary Data S2) from the observed mitochondrial genome arrangements
375 (Fig. 1). Novel tRNA rearrangements observed between the CR and *cox1* in
376 Psocomorpha were treated as missing data for *Stenocaecilius* (Fig. 1).
377 The most parsimonious reconstruction of the condition-based data matrix on the
378 ML phylogenomic tree (Fig. 2) is shown in Fig. 3. The insertions (Character 1–17)
379 contained very little homoplasy (CI = 0.94, RI = 0.98). Translocation of *trnM* was
380 identified as a synapomorphy of *Neotrogla* and *Speleketor*. Both the *Echmepteryx*–
381 *Dorypteryx* clade and the Psocomorpha were characterized by unique gene
382 rearrangements, including a series of non-homoplasious characters (11 and 6
383 respectively). The pattern seen in *Stenocaecilius* (type 6') could be derived by a
384 single tRNA transposition from the psocomorphan type (type 6). The derived gene
385 boundary, *trnI-trnM*, was identified in both *Neotrogla* and the *Echmepteryx*–
386 *Dorypteryx* clade (Character 1), but they were inferred to have independent origins. In
387 comparison, the deletions (Characters A–K) were more homoplasious (CI = 0.79, RI
388 = 0.92). Furthermore, although deletion of *trnM* from its ancestral position (Character
389 B) was identified in almost all taxa except for *Prionoglaris* and was reconstructed to
390 have occurred in the common ancestor of Psocodea, this interpretation is unlikely
391 (see Discussion).
392 Reconstructing the pattern of genome rearrangements using the ALL dataset
393 topology (Fig. 2) in TreeREx recovered the following events between the ancestral
394 pancrustacean mitochondrial genome (including arrangement type 1 *Prionoglaris*)
395 and the 6 derived conditions identified above (Figs 1 and 4):
396 A) a small TDRL involving a 4 gene block (CR to *trnM*) resulting in both the
397 duplication of the CR, and the relative rearrangement of *trnQ* and *trnM* (TDRL I),

in the common ancestor of *Neotrogla* and *Speleketor* (Arrangement types 2 and 3);

B) three rearrangement events including an inversion of *trnI*, transposition of *trnQ*, and a TDRL of an 7 gene block (*trnI* to *trnC*) (TDRL II) in the branch leading to *Speleketor* (Arrangement type 3);

C) an enormous TDRL involving duplication of almost the entire mt genome (33 of 37 genes) and 14 separate block deletions ranging in size from 1 to 9 genes (65 – 5200bp deletions) (TDRL III) in the ancestors of the *Echmepteryx–Dorypteryx* clade (Arrangement type 4) ;

D) a single translocation of *trnM* in the common ancestor of Psocomorpha and Troctomorpha (*Stimulopalpus*) (Arrangment types 5 and 6)

E) a single inversion (*trnI*) in *Stimulopalpus* (Arrangement type 5);

F) two moderate sized TDRLs (TDRL IV 8 genes, TDRL V 4 genes) in the ancestors of the Psocomorpha (Arrangement types 6 and 6');

G) transposition of *trnE* in *Stenocaecilius* (Arrangement type 6').

In addition, there are two possible optimizations for the derived position of *trnM* in the clade *Stimulopalpus*+Psocomorpha (depicted by dotted line in Fig. 4). The transposition of *trnM* could have occurred in the ancestor of this clade or it could have transposed independently in *Stimulopaplus* and as part of the TDRL V event. The number of inferred random losses in TDRL V are the same (4) whether *trnM* was in the insect ancestral genome position or a derived position (*trnI-trnM-trnQ*) prior to this duplication.

4. Discussion

4.1. Mito-phylogenomics

The tree estimated from the mitochondrial genomic data agreed completely with those estimated previously from nuclear and mitochondrial Sanger gene sequencing (Fig. 2: Yoshizawa et al., 2006; Yoshizawa and Johnson, 2010, 2014). Most branches received 100% bootstrap support and posterior probability, except for branches that included taxa with missing data. Tree and support value differences from different data sets were also minimal. In some previous studies, the usefulness of

mitochondrial genomic data for estimating deep insect phylogeny has been questioned (e.g., Cameron et al., 2004 for interordinal relationships). However, for the case of our study of the free-living Psocodea (excluding Liposcelididae), the mitochondrial genome data seems to contain consistent signal for resolving deep phylogenetic relationships between and within suborders.

The only uncertainty and potential conflict with previous studies concerns the monophyly of Prionoglarididae. In a previous analysis, Prionoglaridae was recovered as a monophyletic group (Yoshizawa et al., 2006: fig. 2). However, most of the signal supporting its monophyly was from the nuclear *Histone 3* gene, in which the 3rd codon position shows extremely biased base composition (over 60% AT) for Prionoglarididae species compared to other trogiomorphans (20–34% AT in most cases: Yoshizawa and Johnson, 2010). Therefore, the monophyly of the family recovered in this prior analysis might be an artifact caused by the similarity of base composition. Subsequent analyses with denser taxon and/or gene sampling did not provide support for monophyly of Prionoglarididae (Yoshizawa et al., 2006: fig. 3; Yoshizawa and Johnson, 2014).

In the present analyses, the Prionoglarididae was consistently recovered as a monophyletic group (Fig. 2; Table 2). No obvious directional biases in substitution rate and base composition were identified in the present dataset (Fig. S3, Table S2). Although different datasets provided somewhat variable support values for this clade, they are consistently high. In addition, combining different datasets (e.g., PCG and RNA) provided increased support values (Table 2). Therefore, the mitochondrial data, including the highly variable 3rd codon position, seem to contain consistent signal supporting the monophyly of Prionoglarididae. Alternatively, although monophyly was also supported, support values for Prionoglarididae from the AA data were generally low (Table 2). This pattern of reduced nodal support for the same/highly similar topologies from mitochondrial AA datasets versus nucleotide coding of the same genes has been observed in other insect groups including Polyneoptera (Cameron et al. 2006), Orthoptera (Fenn et al. 2008), and Hymenoptera (Dowton et al. 2009a) and therefore is not surprising at the finer taxonomic scales considered in this study.

4.2. Mitochondrial gene rearrangements

462 Seven types of mitochondrial genome arrangement were identified in the free-
463 living Psocodea studied here (the extensively rearranged and modified mitochondrial
464 genomes of Liposcelididae and Phthiraptera were excluded) (1–6 and 6' in Fig. 1). Of
465 them, the condition identified in *Stenocaecilius* (type 6') can be simply formed from
466 the condition identified in all other Psocomorpha (type 6) by a single rRNA
467 transposition (*trnE*), and thus is regarded here as its sub-category (Fig. 1). Although
468 mitochondrial gene rearrangements are recognized as rare-genomic change events
469 (Boore et al., 1998; Rokas and Holland, 2000) and widely held to not result in
470 homoplasious convergences, a couple of homoplasies were also evident between
471 closely related members of Psocodea. In the following, we evaluate their gene
472 rearrangement history by comparing the results from two different analytical
473 strategies.
474
475 4.2.1. Condition-based coding
476 The condition-based coding method here proposed can handle transpositions,
477 inversions, and inverse-transpositions but cannot recognize more complicated TDRL
478 events as it breaks them up into multiple observed novel gene-boundaries. Character
479 coding and ancestral state reconstruction can be done without any specific
480 mechanistic assumptions as to how genomes rearrange (e.g. the long-running
481 discussion as to whether mitochondrial recombination occurs in animals or not: Mortiz
482 et al. 1987; Dowton & Campbell 2001; Kraytsberg et al. 2004; Ma & O'Farrell, 2015),
483 which can be an advantage of this method. However, if different assumptions about
484 the cause of rearrangements are applied, two alternative character-coding strategies
485 are possible, potentially allowing a test of those assumptions. If deletion and insertion
486 are recognized as simultaneous or a single event (e.g., as would be the case for
487 recombination within a single mitochondrial genome molecule), then either only
488 insertion or only deletion events should be coded. The consequences of such an
489 approach can be seen in Fig. 3, where the insertion and deletion events are
490 separately coded and the utility of each signal type can be clearly assessed. If
491 insertion and deletion are recognized as different evolutionary events (e.g.,
492 recombination between-molecules, which first causes an insertion, then a deletion
493 follows; or as is proposed by the TDRL model), then both insertion and deletion

494 events may be coded. For example, the present analyses recovered possible
495 remnants of the *trnI* and *trnM* genes in their ancestral position flanking *trnQ* in
496 *Neotrogla* (Supplementary Fig. S2). This strongly suggests that the rearrangements
497 in *Neotrogla* were not caused by within-molecule recombination, but rather that the
498 insertions and deletions occurred as different evolutionary events.
499 However, the present results showed that inclusion of deletion characters for the
500 ancestral state estimation is highly problematic, even if between-molecules
501 recombination is an assumed mechanism of rearrangement. First, deletion events are
502 more homoplasious, as has been demonstrated in other insect groups (e.g.
503 Hymenoptera: Dowton et al., 2009b). If gene deletion is random with respect to the
504 newly inserted and original copies, then a half of all deletion events should have
505 occurred in the copy located at the original position. Aside from possibly a stretch of
506 non-coding DNA, deletions of newly inserted genes will not leave any evidence of
507 gene transposition, whereas deletions at the original location will always leave
508 evidence of gene transposition in the form of a novel gene boundary between the
509 genes flanking the deleted one. In addition, while there are 36 possible positions for
510 gene insertions, we observe that some genes rearrange considerably more frequently
511 than others, and thus deletions will cluster on these more mobile genes. For instance
512 within the present set of taxa, *trnM* is rearranged in 5 of the 6 genome arrangement
513 types, resulting in 5 instances of the deletion character state B. These heightened
514 rates of transposition by particular tRNAs have been observed in other taxa giving
515 rise to recognition of rearrangement hotspots (e.g. Dowton and Austin, 1999; Dowton
516 et al., 2003) which are also recognized as sites of convergent rearrangements
517 (Dowton et al., 2009b). Therefore, it is obvious that deletion events at the ancestral
518 location are far more frequently observed than convergent insertion events and thus
519 are more homoplasious.
520 Second and more importantly, homoplasies of deletion characters sometimes
521 can cause very unlikely ancestral state reconstructions. Under both the between-
522 molecules recombination and TDRL scenarios, an insertion event must precede the
523 deletion event. However, for example, as seen in Fig. 3, deletion of *trnM* from
524 between *trnQ* and *nad2* (Character B) is most parsimoniously interpreted to have
525 occurred in the common ancestor of the Psocodea, which was followed by insertions

of *trnM* at multiple different positions in different psocodean lineages: Characters 2, 8, 12 and 15, and reinsertion at its ancestral position in *Prionoglaris* (i.e. reversal of Character B). Therefore, for the most highly supported mitochondrial genome rearrangement models (i.e. between-molecules recombination, TDRL), insertion-only coding provides more accurate ancestral state estimation. If one needs to count the number of actual evolutionary events in the genomic history of a given group, then this can be accomplished by simply doubling the number of insertion events, because deletion events inevitably occurred following the corresponding insertion events.

The mitochondrial genome arrangement of *Prionoglaris* retains the ancestral pancrustacean condition (Fig. 1). Focusing only on the insertion events (i.e., excluding Characters A–K in Fig. 3), four of the five recorded types of novel genome arrangement (2–6 in Fig. 1) were identified as originated independently from the ancestral pancrustacean mitochondrial genome. The majority (10 of 17) of insertion characters are thus autapomorphies. Character 1 (*trnI-trnM*) was homoplasious: it is shared by *Neotrogla* and the *Dorypteryx–Echmepteryx* clade, but their independent origins are quite obvious from the radically different genomic location of the *trnI-trnM* gene pair in these taxa (middle of the CR versus poly-tRNA block between *cox3* and *cox2*, respectively). Only one character (Character 2: *trnM*-CR) was interpreted as a synapomorphic change that groups taxa of different gene arrangement types (2 and 3 in Fig. 1), suggesting multiple rounds of gene rearrangement through time, rather than direct rearrangement from the ancestral pancrustacean mitochondrial genome to the arrangement type seen in these extant genera. Character 2 also supports the close relationship between *Neotrogla* and *Speleketor* (currently grouped in the subfamily Speleketorinae: Lienhard, 2010). Finally, four synapomorphic insertions are identified in the common ancestor of the Psocomorpha (type 6), with only one psocomorphan lineage (*Stenocaecilius*, type 6') having a subsequent rearrangement (Character 17). The type 6' condition was also confirmed recently in a species of Stenopsocidae (*Stenopsocus immaculatus*: Liu et al., 2017), a member of the infraorder Caeciliusetae to which *Stenocaecilius* (Caeciliusidae) is also classified. Therefore, translocation of *trnE* may represent an autapomorphy of the infraorder. The mitochondrial genome of the common ancestor of Psocodea is thus estimated to have retained the pancrustacean ancestral condition. It is also evident from this result

that the extensive rearrangements observed in Psocodea and Thysanoptera have thus occurred independently.

4.2.2. TreeREx analyses

TreeREx software considers tandem-duplication-random-loss (TDRL) as well as transpositions, inversions, and inverted-transpositions (termed 'reverse-transpositions' in the software, however this is less precise and can be misinterpreted as transpositions back to an ancestral gene position, i.e. a character reversal in the cladistics sense). Estimation of TDRL events is much harder to recover without the aid of software like CREx or TreeREx (Bernt et al., 2007, 2008). TDRL events cannot be coded using the condition-based coding method. Because of this difference, the rearrangement histories estimated from the condition-based coding and TreeREx analyses are quite different. However, by both estimations, each type of genome arrangement identified in the free-living Psocodea originated via unique history. The mitochondrial genome arrangement of the common ancestor of Psocodea was estimated to retain the ancestral pancrustacean condition also by TreeREx. By using the condition-based matrix, a single transposition event (Character 2: *trnM*) was identified as synapomorphic between *Speleketor* and *Neotrogla*, and TreeREx also recovered a shared TDRL event between them. TreeREx identified that, from the ancestral condition of *Neotrogla* and *Speleketor* (type 2), the condition of *Speleketor* (type 3) was established by one inversion (*trnI*), one transposition (*trnQ*), and one TDRL (TDRL II: Fig. 1) (see Results). However, the arrangement of *Speleketor* can also be achieved by transposition of *trnC* and inverted-transposition of *trnI* only, without any TDRL event. The former less parsimonious output may potentially be caused by incomplete input data: i.e., duplicated CR in *Speleketor* and *Neotrogla* not coded (Supplementary Data S3).

In contrast, while the condition-based analysis did not recover any shared rearrangement event between *Stimulopalpus* and Psocomorpha, TreeREx recovered a transposition of *trnM* as a shared event. However, there is also an equally parsimonious scenario: occurrence of transposition of *trnM* in *Stimulopalpus*, while TDRL V from the ancestral insect genome arrangement (Fig. 1) in Psocomorpha can also explain the final arrangement types with exactly the same numbers of

transposition (1), tandem duplication (1) and independent loss (4) events.

4.2.3. Conclusion

Both methods (character-based coding and TreeREx) provided similar conclusions for the ancestral states of the mitochondrial genome arrangement (Figs 3–4). The effectiveness of these methods cannot be compared directly (e.g. comparing identified number of events by a parsimony criterion) because the different methods use different assumptions for the mechanism of mitochondrial gene rearrangements. Nevertheless, as mentioned above, incorporation of deletion characters into the condition-based matrix involves higher risk of inferring incorrect historical reconstructions and thus should be avoided regardless of the assumed evolutionary mechanisms. The character-based coding method is straightforward, and the constructed matrix can be used directly for ancestral state reconstruction, which provided quite reasonable conclusions in the present case. Each character in the matrix can be considered as an evolutionary event so that the data matrix constructed by the condition-based coding can also be used for phylogenetic estimation. A drawback of the condition-based coding is that it cannot handle TDRL events.

In contrast, TreeREx considers TDRL as well and estimates the rearrangement history directly from the gene order data, without specific character coding. The present analyses, however, recovered some potential flaws of the present TreeREx algorithm. First, TreeREx does not allow the existence of duplicated gene in the input data. Possibly because of this, an apparently less-parsimonious interpretation was obtained for the rearrangement history of *Speleketor*. In addition, TreeREx only outputs a single result, even if there are equally parsimonious possibilities (TreeREx output ACCTRAN-type reconstruction, although DELTRAN-type reconstruction is also possible for the transposition of *trnM* in *Stimulopalpus* and Psocomorpha: Fig. 4). Such possibilities must be manually examined based on the phylogenetic relationships and TreeREx output.

Plausibility of different mechanistic assumptions should also be evaluated, not only by parsimony criterion, but also by detailed mitochondrial genome analyses, with dense taxon sampling and strong phylogenetic backbone. Previous evidence has

favored the TDRL model (Dowton et al., 2009; Beckenbach, 2011) but, in the present case, the inversion of *trnI* cannot be explained by TDRL. Alternatively, the presence of a potential *trnI* remnant in *Neotrogla* cannot be explained by within-molecule recombination. The between-molecule recombination model can explain both, but this does not overwhelmingly favor that model because each rearrangement event might have been caused by different mechanisms. The present study showed that more highly rearranged mitochondrial genomes can still be quite consistent within higher taxa (i.e., *Echmepteryx–Dorypteryx* clade which includes all trogiomorphs except Prionoglarididae, and Psocomorpha from which all major clades were sampled). Therefore, their intermediate genome arrangements cannot be recovered from the extant species. In contrast, variation was identified within the family Prionoglarididae. Only three representatives of Prionoglarididae were included in the present analyses, and there are more genera not analyzed here (e.g., *Sensitibilla* and *Afrotrogla* considered close to *Neotrogla*, and *Siamoglaris* and *Speleopsocus* considered close to *Prionoglaris*) each of which includes multiple species (except for the monotypic *Speleopsocus*). In addition, only a single species (*Stimulopalpus*) was analyzed from the primitive members of the suborder Troctomorpha (i.e., excluding highly derived Liposcelididae), although there are seven more families in this group. Analyses of these taxa may provide further clues to evaluate mitochondrial rearrangement history and mechanisms in the Psocodea.

Acknowledgments

We thank Nico Schneider for supplying valuable specimens. This project was supported by JSPS Grant (15H04409) to KY, the US National Science Foundation (DEB0444972), CSIRO Julius Career Awards, and the Australian Research Council Future Fellowships scheme (FT120100746) to SLC, and NSF DEB-1239788 and DEB-1342604 to KPJ.

References

653 Allen, J.M., Huang, D.I., Cronk, Q.C., Johnson, K.P., 2015. aTRAM – automated target
654 restricted assembly method: a fast method for assembling lici across divergent taxa
655 from next-generation sequencing data. BMC Bioinfomatics 16, 98.
656 Andujar, C., Arribas, P., Linard, B., KUndrata, R., Bocak, L., Vogler, A.P., 2017. The
657 mitochondrial genome of *Iberobaenia* (Coleoptera: Iberobaeniidae): first
658 rearrangement of protein-coding genes in the beetles. Mitochondrial DNA Part A 28,
659 156–158.
660 Beckenbach, A.T., 2011. Mitochondrial genome sequences of representatives of three
661 families of scorpionflies (Order Mecoptera) and evolution in a major duplication of
662 coding sequence. Genome 54, 368–376.
663 Beckenbach, A.T., 2012. Mitochondrial genome sequences of Nematocera (Lower Diptera):
664 evidence of rearrangement following a complete genome duplication in a winter crane
665 fly. Genome Biol. Evol. 4, 89–101.
666 Bern, M., Merkle, D., Ramsch, K., Fritzsch, G., Perseke, M., Bernhard, D., Schlegel, M.,
667 Stadler, P.F., Middendorf, M., 2007. CREx: inferring genomic rearrangements based
668 on common intervals. Bioinformatics 23, 2957–2958.
669 Bernt, M., Merkle, D., Middendorf, M., 2008. An algorithm for inferring mitogenome
670 rearrangements in a phylogenetic tree. In: Nelson, C.E., Vialette, S. (Eds.),
671 Comparative Genomics. RECOMB-CG 2008. Lecture Notes in Computer Science, vol.
672 5267. Springer, Berlin, pp. 143–157.
673 Bernt, M., Donath, A., Jühling, F., Externbrink, F., Florentz, C., Fritzsch, G., Pütz, J.,
674 Middendorf, M., Stadler, P.F., 2013. MITOS: Improved *de novo* metaxoan
675 mitochondrial genome annotation. Mol. Phylogenet. Evol. 69, 313–319.
676 Boore, J.L., Lavrov, D.V., Brown, W.M., 1998. Gene translocation links insects and
677 crustaceans. Nature 392, 667–668.
678 Boore JL. 2000. The duplication random-loss model for gene rearrangement exemplified by
679 mitochondrial genomes of deuterosome animals. In *Comparative Genomics: Empirical*
680 *and analytical approaches to gene order dynamics, map alignment and the evolution*
681 *of gene families*, eds D Sankoff, JH Nadeau, pp. 133-48. Dordrecht: Kluwer Academic
682 Publishers.
683 Cameron, S.L., 2014a. Insect mitochondrial genomics: implications for evolution and
684 phylogeny. Ann. Rev. Entomol. 59, 95–117.

685 Cameron, S.L., 2014b. How to sequence and annotate insect mitochondrial genomes for
686 systematic and comparative genomics research. Syst. Entomol. 39, 400–411.
687 Cameron, S.L., Miller, K.B., D'Haese, C.A., Whiting, M.F., Barker, S.C., 2004.
688 Mitochondrial genome data alone are not enough to unambiguously resolve the
689 relationship of Entognatha, Insecta and Crustacea. Cladistics 20, 534–557.
690 Cameron, S.L., Barker, S.C. & Whiting, M.F. 2006. Mitochondrial genomics and the
691 relationships and validity of the new insect order Mantophasmatodea. Mol.
692 Phylogenet. Evol. 38: 274-279.
693 Cameron, S.L., Yoshizawa, K., Mizukoshi, A., Whiting, M.D., Johnson, K.P., 2011.
694 Mitochondrial genome deletions and mini-circles are common in lice (Insecta:
695 Phthiraptera). BMC Genomics 12: 394.
696 Chen, S.C., Wei, D.D., Shao, R., Shi, J.X., DouW., Wang, J.J., 2014. Evolution of
697 multipartite mitochondrial genomes in the booklice of the genus *Liposcelis*
698 (Psocoptera). BMC Genomics 15, 861.
699 Dickey, A.M., Kumar, V., Morgan, J.K., Jara-Cavieres, A., Shatters Jr., R.G., Mckenzie,
700 C.L., Osborne, L.S., 2015. A novel mitochondrial genome architecture in thrips
701 (Insecta: Thysanoptera): extreme size asymmetry among chromosomes and possible
702 recent control region duplication. BMC Genom. 16, 439.
703 Dowton, M., Austin, A.D., 1999. Evolutionary dynamics of a mitochondrial rearrangement
704 "hot spot" in the Hymenoptera. Mol. Biol. Evol. 16, 298–309.
705 Dowton M, Campbell NJH. 2001. Intramitochondrial recombination – is it why some
706 mitochondrial genes sleep around? Trends Ecol. Evol. 16: 269-271.
707 Dowton, M., Castro, L.R., Campbell, S.L., Bargon, S.D., Austin, A.D., 2003. Frequent
708 mitochondrial gene rearrangement at the hymenopteran nad3–nad5 junction. J. Mol.
709 Evol. 56, 517–526.
710 Dowton, M., Cameron, S.L, Austin, A.D. & Whiting, M.F. 2009. Phylogenetic approaches
711 for the analysis of mitochondrial genome sequence data in the Hymenoptera – a
712 lineage with both rapidly and slowly evolving mitochondrial genomes. Mol.
713 Phylogenet. Evol. 52: 512-519
714 Dowton, M., Cameron, S.L., Dowavic, J.I., Austin, A.D., Whiting, M.F., 2009b.
715 Characterization of 67 mitochondrial tRNA gene rearrangements in the Hymenoptera

716 suggests that mitochondrial tRNA gene position is selectively neutral. Mol. Biol. Evol.
717 26, 1607–1617.
718 Edgar, R.C., 2004. MUSCLE: multiple sequence alignment with high accuracy and high
719 throughput. Nucletic Acids Res. 32, 1792–1797.
720 Fenn, J.D., Song, H., Cameron, S.L. & Whiting, M.F. 2008. A mitochondrial genome
721 phylogeny of Orthoptera (Insecta) and approaches to maximizing phylogenetic signal
722 found within mitochondrial genome data. Mol. Phylogenet. Evol. 49: 59-68.
723 Hahn, C., Bachmann, L., Chevreux, B., 2013. Reconstructing mitochondrial genomes directly
724 from genomic next-generation sequencing reads – a baiting and iterative mapping
725 approach. Nuc. Acid. Res. 41, e129.
726 Katoh, K., Standley, D.M., 2013. MAFFT Multiple Sequence Alignment Software version 7:
727 improvement in performance and usability. Mol. Biol. Evol. 30, 772–780.
728 Kômoto, N., Yukuhiro, K., Tomita, S., 2012. Novel gene rearrangements in the
729 mitochondrial genome of a webspinner, *Aposthonia japonica* (Insecta: Embioptera).
730 Genome 55, 222–233.
731 Kumar, S., Stecher, G., Tamura, K., 2016. MEGA7: Molecular evolutionary genetics analysis
732 version 7.0 for bigger datasets. Mol. Biol. Evol. 33, 1870–1874.
733 Kraytsberg, Y., Schwartz, M., Brown, T.A., Ebralidse, K., Kunz, W.S., Clayton, D.A.,
734 Vissing, J., Khrapko, K. 2004. Recombination of human mitochondrial DNA. *Science*
735 304: 981.
736 Lanfear, R., Frandsen, P.B., Wright, A.M., Senfeld, T., Calcott, B., 2017. PartitionFinder 2:
737 New methods for selecting partitioned models of evolution for molecular and
738 morphological phylogenetic analyses. Mol. Biol. Evol. 34, 772–773.
739 Lartillot, N., Lepage, T., Blanquart, S., 2009. PhyloBayes 3: a Bayesian software package for
740 phylogenetic reconstruction and molecular dating. Bioinformatics 25, 2286–2288.
741 Li, H, Liu, H, Shi, A., Stys, P., Zhou, X., Cai, W. 2012. The complete mitochondrial genome
742 and novel gene arrangement of the unique headed bug *Stenopirates* sp. (Hemiptera:
743 Enicocephalidae). PLoS ONE 7, 29419.
744 Li, H., Shao, R., Song, F., Zhou, X., Yang, Q., Li, Z., Cai, W., 2013. Mitochondrial genomes
745 of two barklice, *Psococerastis albimaculata* and *Longivalvus hyalospilus* (Psocoptera:
746 Psocomorpha): contrasting rates in mitochondrial gene rearrangement between major
747 lineages of Psocodea. PLoS ONE 8, e61685.

748 Lienhard, C., 1998. Psocoptères euro-méditerranèens. Faune de France 83, Fédération
749 Française des Sociétés de Sciences naturelles, Paris.
750 Lienhard, C., 2010. A new genus of Sensitibillini from Brazilian caves (Psocodea:
751 'Psocoptera': Prionoglarididae). Rev. Suisse Zool. 117, 611–635.
752 Linard, B., Crampton-Platt, A., Gillett, C.P.D.T., Timmermans, M.J.T.N., Vogler, A.P., 2015.
753 Metagenome skimming of insect specimen pools: potential for comparative genomics.
754 Genome Biol. Evol. 7, 1474–1489.
755 Liu, H., Li, H., Cai, Y., Song, F., Wilson, J.J., Cai, W., 2017. Conserved gene arrangement in
756 the mitochondrial genomes of barklouse families Stenopsocidae and Psocidae. Front.
757 Agr. Sci. Eng. 4, 358–365.
758 Liu, H., Li, H., Song, F., Gu, W., Feng, J., Cai, W., Shao, R., 2017. Novel insignts into
759 mitochondrial gene rearrangement in thrips (Insecta: Thysanoptera) from the grass
760 thrips, *Anaphothrips obscurus*. Sci Rep 7, 4284.
761 Ma, H., O'Farrell, P.H. 2015. Selections that isolate recombinant mitochondrial genomes in
762 animals. eLife 4: e07247.
763 Maddison, D.R., Maddison, W.P., 2000. MacClade 4: Analysis of Phylogeny and Character
764 Evolution. Sinauer Assoc., Sunderland, MA.
765 Mao, M., Gibson, T., Dowton, M., 2015. Higher-level phylogeny of the Hymenoptera
766 inferred from mitochondrial genomes. Mol. Phylogenet. Evol. 84, 34–43.
767 Moritz C., Dowling, T.E., Brown, W.M., 1987. Evolution of animal mitochondrial DNA:
768 relevance for population biology and systematics. Ann. Rev. Ecol. Syst. 18: 269-292.
769 Nguyen, L.T., Schmidt, H.A., von Haeseler, A., Minh, B.Q., 2015. IQ-TREE: A fast and
770 effective stochastic algorithm for estimating maximum-likelihood phylogenies. Mol.
771 Biol. Evol. 32, 268–274.
772 Rokas, A., Holland, P.W.H., 2000. Rare genomic changes as a tool for phylogenetics. Trends
773 Ecol. Evol. 15, 454–459.
774 Ronquist, F., Huelsenbeck, J.P., 2003. MrBayes 3: Bayesian phylogenetic inference under
775 mixed model. Bioinformatics 19, 1572–1574.
776 Shao, R., Barker, S.C., 2003. The highly rearranged mitochondrial genome of the plague
777 thrips, *Thrips imaginis* (Insecta: Thysanoptera): convergence of two novel gene
778 boundaries and an extraordinary arrangement of rRNA genes. Mol. Biol. Evol. 20,
779 362–370.

780 Shao, R., Campbell, N.J.H., Barker, S.C., 2001a. Numerous gene rearrangements in the
781 mitochondrial genome of the wallaby louse, *Heterodoxus macropus* (Phthiraptera).
782 Mol. Biol. Evol. 18, 858–865.
783 Shao, R., Campbell, N.J.H., Schmidt, E.R., Barker, S.C., 2001b. Increased rate of gene
784 rearrangement in the mitochondrial genomes of three orders of hemipteroid insects.
785 Mol. Biol. Evol. 18, 1828–1832.
786 Shao, R., Dowton, M., Murrell, A., Barker, S.C., 2003. Rates of gene rearrangement and
787 nucleotide substitution are correlated in the mitochondrial genomes of insects. Mol.
788 Biol. Evol. 20, 1612–1619.
789 Shao, R., Kirkness, E.F., Barker, S.C., 2009. The single mitochondrial chromosome typical
790 of animals has evolved into 18 minichromosomes in the human body louse, *Pediculus*
791 *humanus*. Genome Res. 19, 904–912.
792 Shao, R., Barker, S.C., Li, H., Song, S., Poudel, S., Su, Y., 2015. Fragmented mitochondrial
793 genomes in two suborders of parasitic lice of eutherian mammals (Anoplura and
794 Rhynchophthirina, Insecta). Sci. Rep. 5, 17389.
795 Shao, R., Li, H., Barker, S.C., Song, S., 2017. The mitochondrial genome of the guanaco
796 louse, *Microthoracius praelongiceps*: insights into the ancestral mitochondrial
797 karyotype of sucking lice (Anoplura, Insecta). Genome Biol. Evol. 9, 431–445.
798 Shi, Y., Chu, Q., Wei, D.D., Qiu, Y.J., Shang, F., Dou, W., Wang, J.J., 2016. The
799 mitochondrial genome of booklouse, *Liposcelis sculptilis* (Psocoptera: Liposcelididae)
800 and the evolutionary timescale of *Liposcelis*. Sci. Rep. 6, 30660.
801 Simpson, J.T., Wong, K., Jackman, S.D., Schein, J.E., Jones, S.J.M., Birol, I., 2009. ABySS:
802 A parallel assembler for short read sequence data. Genome Res. 19, 1117–1123.
803 Swofford, D.L., 2002. PAUP*. Phylogenetic Analysis Using Parsimony (* and Other
804 Methods). Version 4. Sinauer Assoc., Sunderland, MA.
805 Yan, D., Tang, Y., Hu, M., Liu, F., Zhang, D., Fan, J., 2012. The mitochondrial genome of
806 *Frankliniella intonsa*: Insights into the evolution of mitochondrial genomes at lower
807 taxonomic levels in Thysanoptera. Genomics 104, 306–312.
808 Yoshizawa, K., Johnson, K.P., 2006. Morphology of male genitalia in lice and their relatives
809 and phylogenetic implications. Syst. Entomol. 31, 350–361.

Yoshizawa, K., Johnson, K.P., 2010. How stable is the ‘‘Polyphyly of Lice” hypothesis?: a comparison of phylogenetic signal in multiple genes. Mol. Phylogenet. Evol. 55, 939–951.

Yoshizawa, K., Johnson, K.P., 2014. Phylogeny of the suborder Psocomorpha (Insecta: Psocodea: 'Psocoptera'): congruence and incongruence between morphology and molecules. Zool. J. Linn. Soc. 171, 716–731.

Yoshizawa, K., Lienhard, C., 2010. In search of the sister group of the true lice: A systematic review of booklice and their relatives, with an updated checklist of Liposcelididae (Insecta: Psocodea). Arthropod Syst. Phylog. 68, 181–195.

Yoshizawa, K., Lienhard, C., 2016. Bridging the gap between chewing and sucking in the hemipteroid insects: new insights from Cretaceous amber. Zootaxa 4079, 229–245.

Yoshizawa, K., Lienhard, C., Johnson, K.P., 2006. Molecular systematics of the suborder Trogiomorpha (Insecta: Psocodea: ‘Psocoptera’). Zool. J. Linn. Soc. 146, 287–299.

Captions

Fig. 1. Seven types of the mitochondrial gene arrangements detected from "Psocoptera". Numbers indicate novel gene boundary possibly caused by insertion events, whereas alphabets indicate possible deletion events (condition-based coding: see Fig. 3). Red dotted lines under genome map indicate tandem-duplication-random-loss events (TDRL) identified by TreeREx analysis (see Fig. 4).

Fig. 2. Mitochondrial phylogeny of the "Psocoptera" estimated from ALL dataset. Numbers associated with branches indicate bootstrap/posterior probability values estimated from this data set. Support values for Prionoglarididae estimated from other datasets are provided in Table 2.

Fig. 3. Most parsimonious reconstruction of the condition-based coding data of the mitochondrial gene arrangements. Numbers (gain condition, filled square or triangle) and alphabets (loss condition, open square or triangle) on branches corresponds those scored in Fig.1. Square indicates non-homoplasious condition whereas triangle indicates homoplasious condition. Numbers associated to taxa corresponds the gene arrangement types in Fig. 1.

Fig. 4. Gene rearrangement history as estimated by TreeREx software. See Result section for detailed rearrangement events. Equally parsimonious interpretations are indicated by gray dotted line. A–E correspond to evolutionary events discussed in the text. Abbreviations: Inv.–inversion; TD–tandem duplication; Trans–transposition.

Table 1. List of taxa analyzed in this study, with GenBank accession numbers

Table 2. Support values for Prionoglarididae estimated from different gene and taxon sets with different analytical methods.

Supplements

Data S1. Nexus file of aligned mitochondrial data.

Data S2. Nexus file of the condition-base coding data of gene arrangements.

Data S3. Input data for the TreeREx analysis. Taxa showing the identical genome arrangement were treated as a single terminal taxon.

856 Table S1. Primers used for long PCR.

857 Table S2. Gene annotations.

858 Table S3. AT-content of each gene/taxon.

859 Fig. S1. Repeat units between *trnM* and -*trnQ* of *Neotrogla*.

860 Fig. S2. Hairpin structure between *trnI* anticodon arm and potential *trnI* ruminant
861 detected in *Neotrogla*.

862 Fig. S3. Plots of p-distance calculated from different data sets (taxa with missing data
863 excluded)

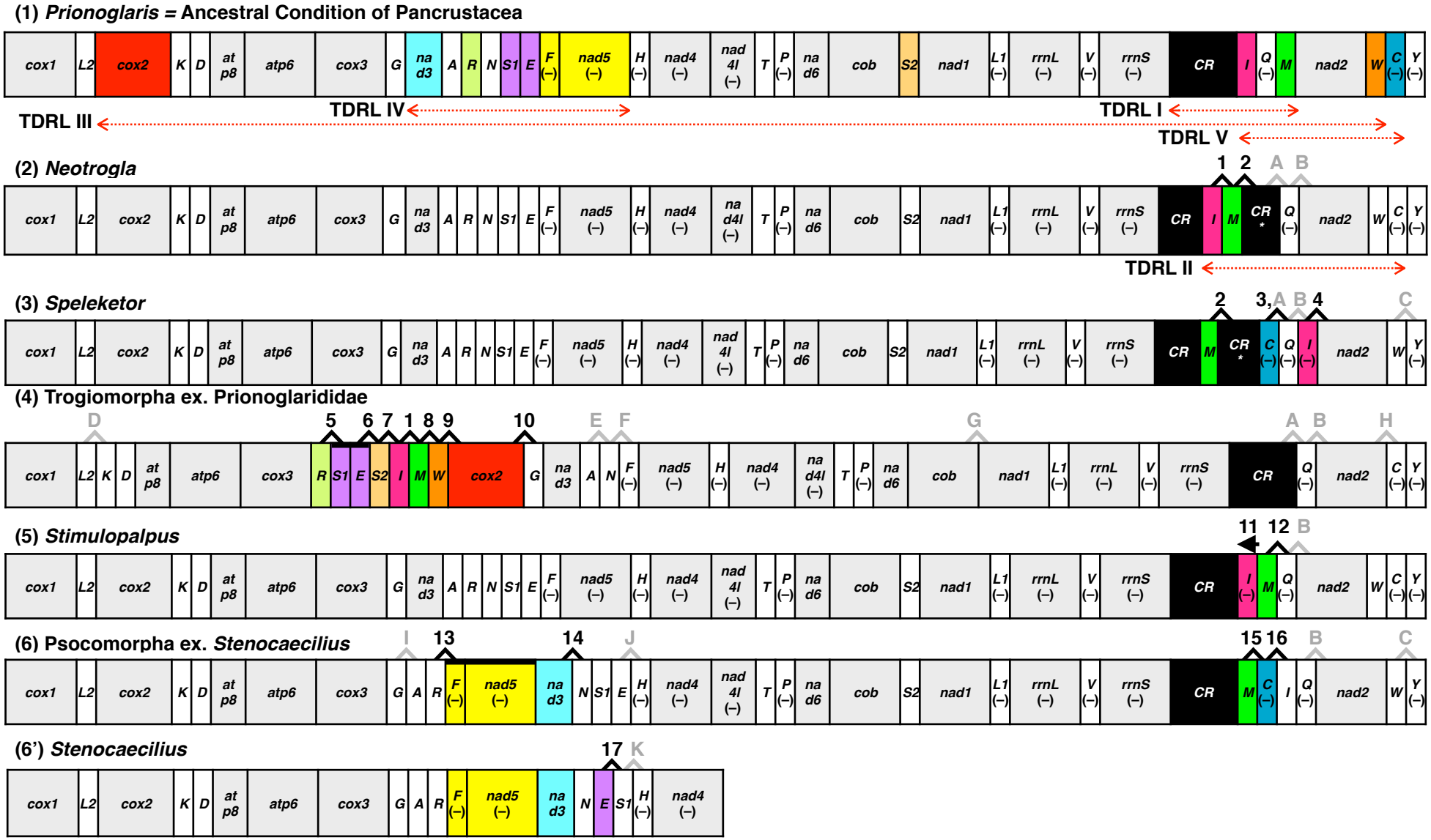
(1) Prionoglaris = Ancestral Condition of Pancrustacea
cox1 L2 cox2 K D atp8 atp6 cox3 G nad3 A R N S1 E F(–) nad5(–) H(–) nad4(–) nad4l(–) T P(–) nad6 cob S2 nad1 L1(–) rrnL(–) V(–) rrnS(–) CR I Q(–) M nad2 W C(–) Y(–)
TDRL III
TDRL IV
TDRL I
TDRL V
(2) Neotrogla
1 2 A B
cox1 L2 cox2 K D atp8 atp6 cox3 G nad3 A R N S1 E F(–) nad5(–) H(–) nad4(–) nad4l(–) T P(–) nad6 cob S2 nad1 L1(–) rrnL(–) V(–) rrnS(–) CR I M CR* Q(–) nad2 W C(–) Y(–)
TDRL II
(3) Speleketor
2 3, A B 4 C
cox1 L2 cox2 K D atp8 atp6 cox3 G nad3 A R N S1 E F(–) nad5(–) H(–) nad4(–) nad4l(–) T P(–) nad6 cob S2 nad1 L1(–) rrnL(–) V(–) rrnS(–) CR M CR* C(–) Q(–) I(–) nad2 W Y(–)
(4) Trogiomorpha ex. Prionoglarididae
D 5 6 7 1 8 9 10 E F G A B H
cox1 L2 K D atp8 atp6 cox3 R S1 E S2 I M W cox2 G nad3 A N F(–) nad5(–) H(–) nad4(–) nad4l(–) T P(–) nad6 cob nad1 L1(–) rrnL(–) V(–) rrnS(–) CR Q(–) nad2 C(–) Y(–)
(5) Stimulopalpus
11 12 B
cox1 L2 cox2 K D atp8 atp6 cox3 G nad3 A R N S1 E F(–) nad5(–) H(–) nad4(–) nad4l(–) T P(–) nad6 cob S2 nad1 L1(–) rrnL(–) V(–) rrnS(–) CR I(–) M Q(–) nad2 W C(–) Y(–)
(6) Psocomorpha ex. Stenocaecilius
I 13 14 J 15 16 B C
cox1 L2 cox2 K D atp8 atp6 cox3 G A R F(–) nad5(–) nad3 N S1 E H(–) nad4(–) nad4l(–) T P(–) nad6 cob S2 nad1 L1(–) rrnL(–) V(–) rrnS(–) CR M C(–) I Q(–) nad2 W Y(–)
(6') Stenocaecilius
17 K
cox1 L2 cox2 K D atp8 atp6 cox3 G A R F(–) nad5(–) nad3 N E S1 H(–) nad4(–)

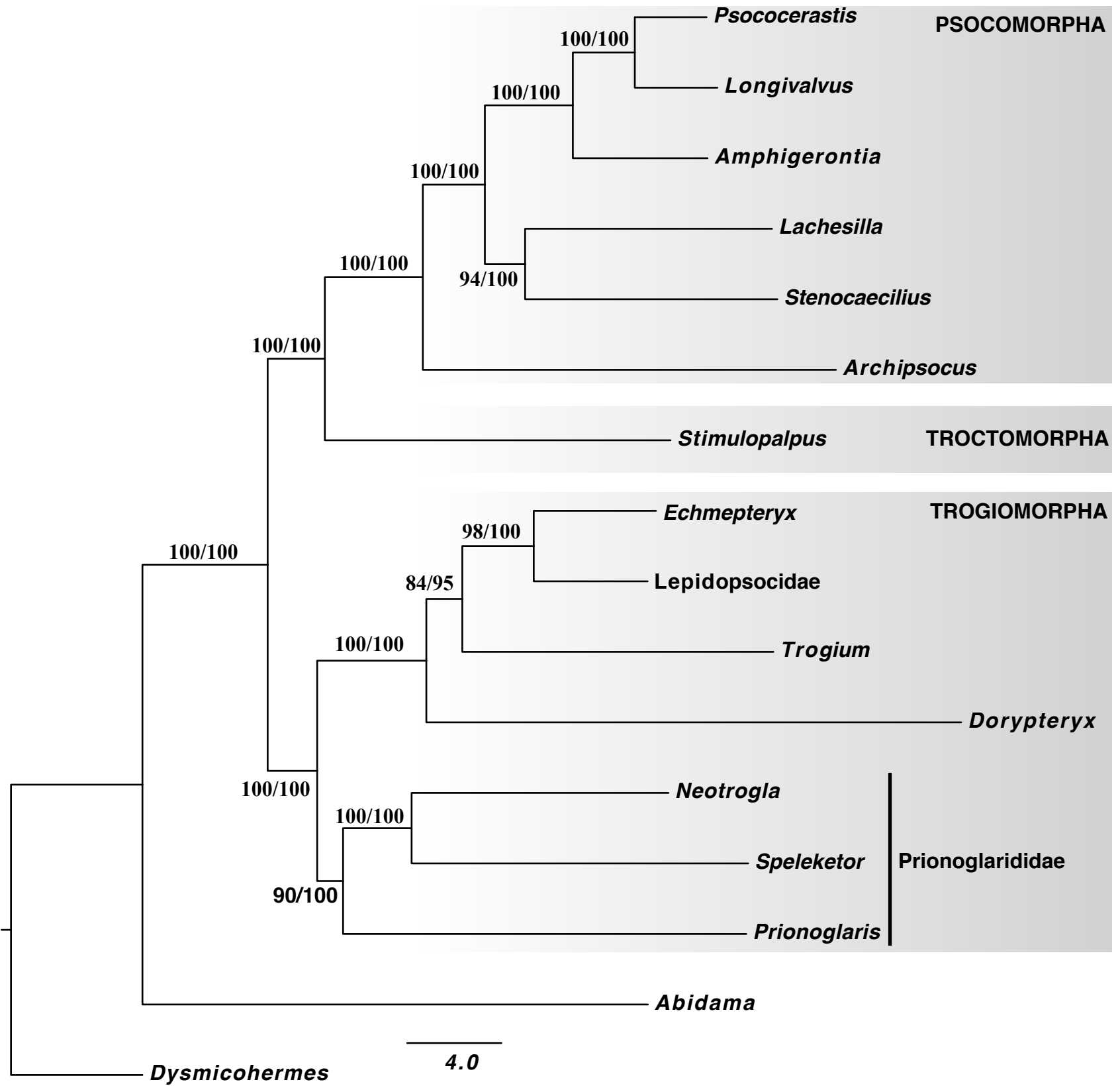
Psococerastis
PSOCOMORPHA
100/100
Longivalvus
100/100
Amphigerontia
100/100
Lachesilla
100/100
94/100
Stenocaecilius
100/100
Archipsocus
Stimulopalpus
TROCTOMORPHA
TROGIOMORPHA
Echmepteryx
98/100
100/100
Lepidopsocidae
84/95
100/100
Trogium
Dorypteryx
100/100
Neotrogla
100/100
Speleketor
Prionoglarididae
90/100
Prionoglaris
Abidama
4.0
Dysmicohermes

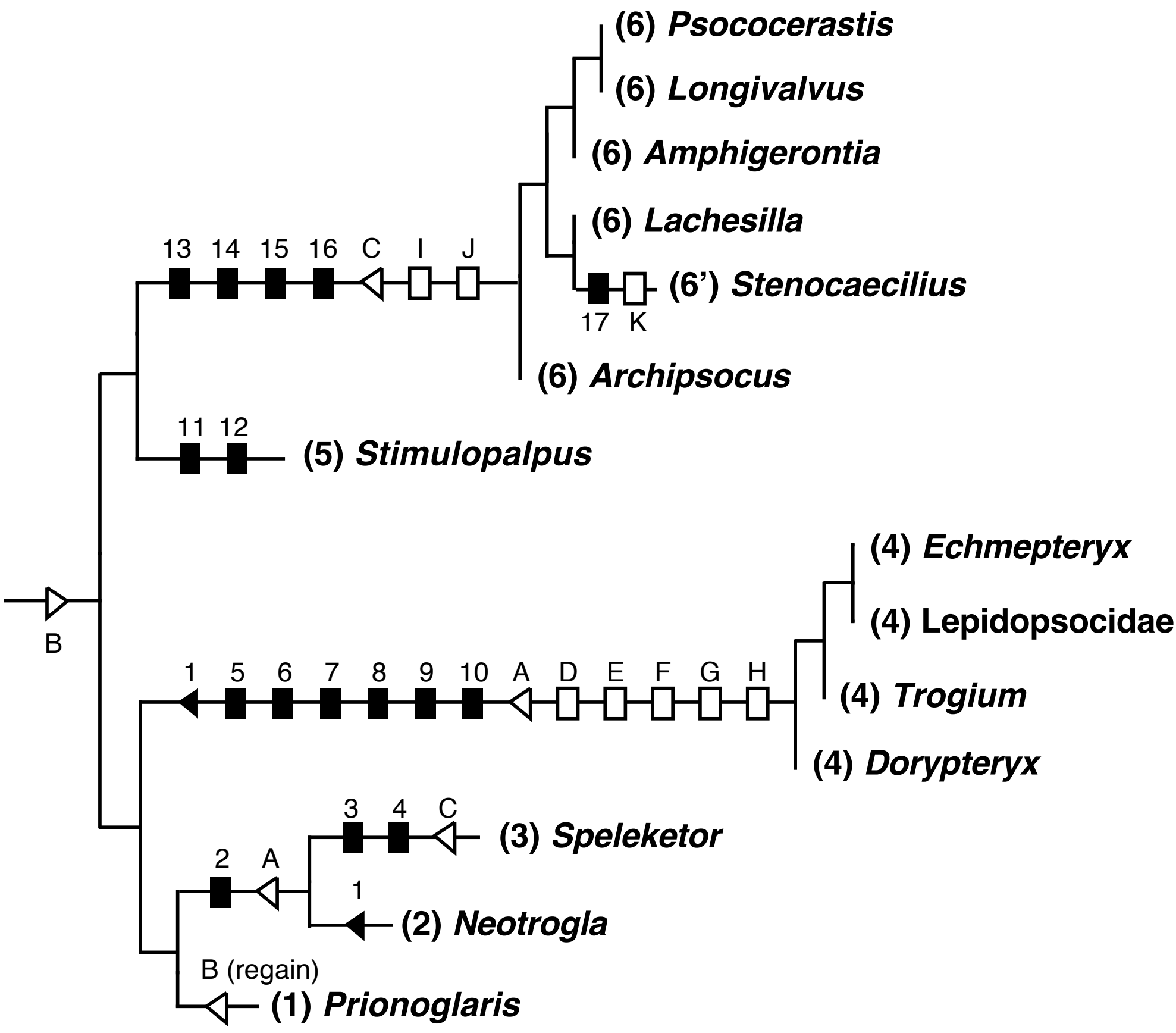
(6) Psococerastis
(6) Longivalvus
(6) Amphigerontia
(6) Lachesilla
13 14 15 16 C I J
(6') Stenocaecilius
17 K
(6) Archipsocus
11 12
(5) Stimulopalpus
(4) Echmepteryx
(4) Lepidopsocidae
B
1 5 6 7 8 9 10 A D E F G H
(4) Trogium
(4) Dorypteryx
3 4 C
(3) Speleketor
2 A
1
(2) Neotrogla
B (regain)
(1) Prionoglaris

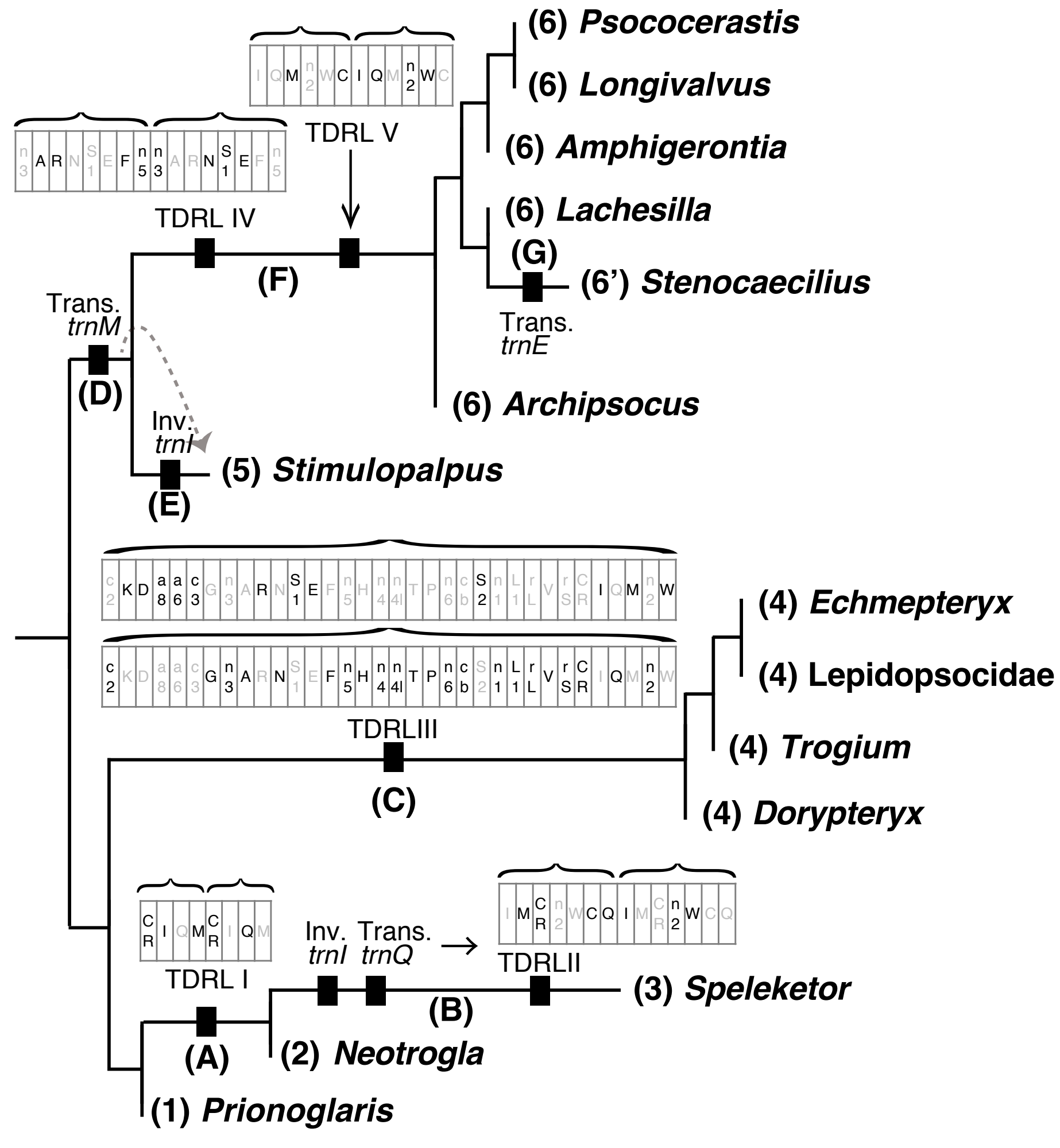
(6) Psococerastis
(6) Longivalvus
(6) Amphigerontia
(6) Lachesilla
(G)
(6') Stenocaecilius
Trans. trnE
(6) Archipsocus
TDRL V
TDRL IV
(F)
Trans. trnM
(D)
Inv. trnI
(5) Stimulopalpus
(E)
(4) Echmepteryx
(4) Lepidopsocidae
(4) Trogium
(4) Dorypteryx
TDRLIII
(C)
Inv. trnI
Trans. trnQ
TDRLII
(3) Speleketor
(B)
TDRL I
(A)
(2) Neotrogla
(1) Prionoglaris

Table 1. List of taxa analyzed in this study, with GenBank accession numbers

Order	Suborder	Family	Genus	Species	Locality	GenBank #
Psocodea	Trogiomorpha	Prionoglarididae	*Prionoglaris*	*stygia*	Luxembourg	given upon acceptance
			Neotrogla	sp.	Brazil: Minas Gerais	given upon acceptance
			Speleketor	*irwini*	USA: California	given upon acceptance
		Psyllipsocidae	*Dorypteryx*	*domestica*	Switzerland: Geneva	given upon acceptance
		Trogiidae	*Trogium*	*pulsatorium*	United Kingdom: Sussex	given upon acceptance
		Lepidopsocidae	*Genus*	sp.	GenBank	NC004816
			Echmepteryx	*hageni*	USA: Illinois	given upon acceptance
	Troctomorpha	Amphientomidae	*Stimulopalpus*	*japonicus*	USA: Illinois	given upon acceptance
	Psocomorpha	Archipsocidae	*Archipsocus*	*nomas*	USA: Florida	given upon acceptance
		Caeciliusidae	*Stenocaecilius*	*quercus*	GenBank	AH010776.3
		Lachesillidae	*Lachesilla*	*anna*	USA: Illinois	given upon acceptance
		Psocidae	*Amphigerontia*	*montivaga*	USA: Arizona	given upon acceptance
			Psococerastis	*albimaculata*	GenBank	JQ910989
			Longivalvus	*hyalospilus*	GenBank	JQ910986
Hemiptera	Auchenorrhyncha	Cercopidae	*Abidama*	*producta*	GenBank	GQ337955
Megaloptera	–	Corydalidae	*Dysmicohermes*	*ingens*	GenBank	KJ806318

taxon\data set	All	ex.3rd	RNA	PCG	PCG12	AA
MrBayes_Full	100	100	100	99.4	98.1	98.8
exMissing	100	100	100	99.6	98.7	100
IQtree_Full	90	93	88	72	70	56
exMissing	90	91	81	75	75	70
PhyloBayes_Full	99	99	99	86	80	62

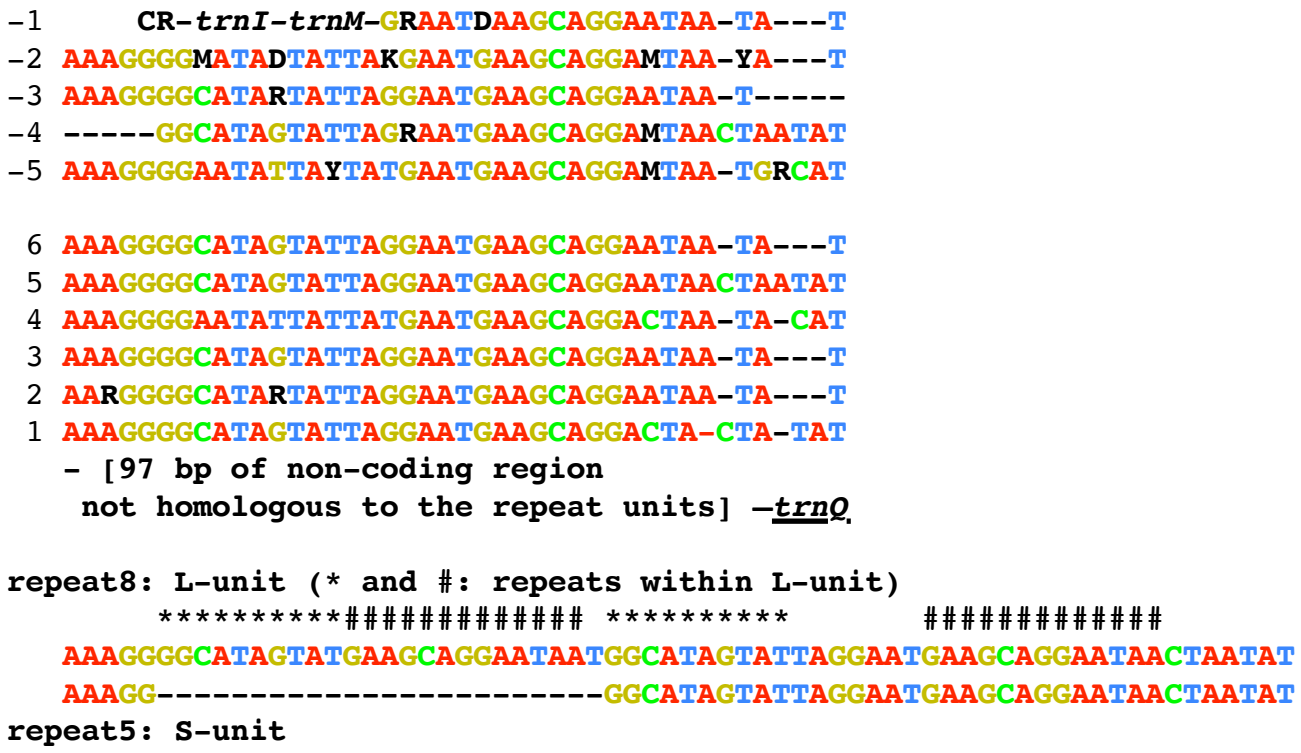
-1 CR-trnI-trnM-GRAATDAAGCAGGAATAA-TA---T
-2 AAAGGGGMATADTATTAKGAATGAAGCAGGAMTAA-YA---T
-3 AAAGGGGCATARTATTAGGAATGAAGCAGGAATAA-T-----
-4 -----GGCATAGTATTAGRAATGAAGCAGGAMTAACTAATAT
-5 AAAGGGGAATATTAYTATGAATGAAGCAGGAMTAA-TGRCAT
6 AAAGGGGCATAGTATTAGGAATGAAGCAGGAATAA-TA---T
5 AAAGGGGCATAGTATTAGGAATGAAGCAGGAATAACTAATAT
4 AAAGGGGAATATTATTATGAATGAAGCAGGACTAA-TA-CAT
3 AAAGGGGCATAGTATTAGGAATGAAGCAGGAATAA-TA---T
2 AARGGGGCATARTATTAGGAATGAAGCAGGAATAA-TA---T
1 AAAGGGGCATAGTATTAGGAATGAAGCAGGACTA-CTA-TAT
- [97 bp of non-coding region
not homologous to the repeat units] —trnQ
repeat8: L-unit (* and #: repeats within L-unit)
********** ********** ##########
AAAGGGGCATAGTATGAAGCAGGAATAATGGCATAGTATTAGGAATGAAGCAGGAATAACTAATAT
AAAGG----------GGCATAGTATTAGGAATGAAGCAGGAATAACTAATAT
repeat5: S-unit

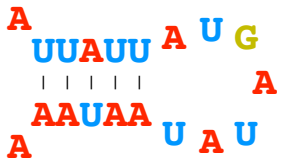

anticodon arm of *trnI*

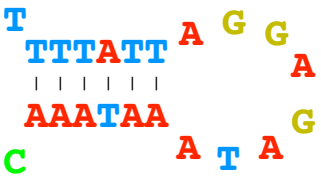

potential remnant of *trnI*

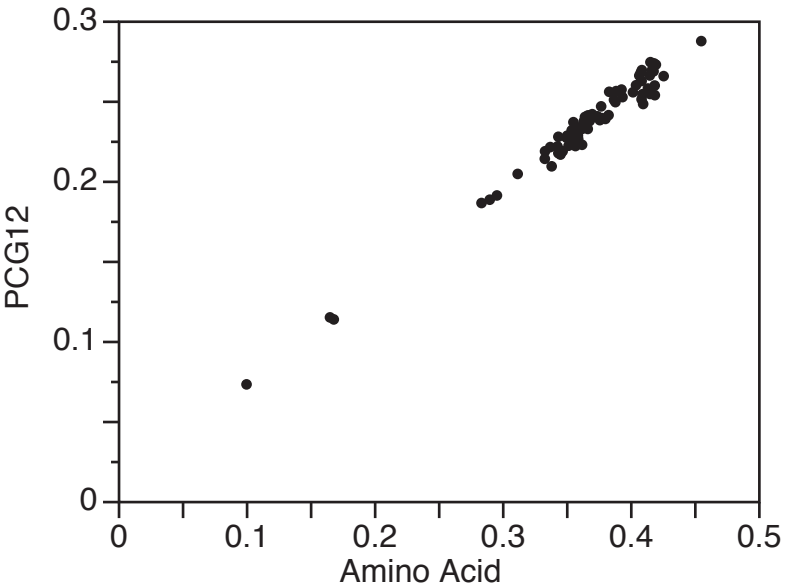
PCG12
Amino Acid
0
0.1
0.2
0.3
0.4
0.5

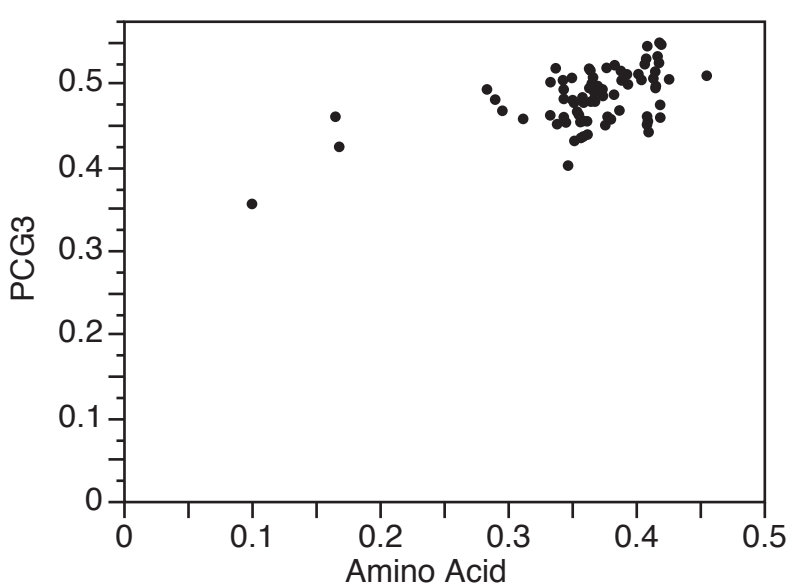
PCG3
Amino Acid
0
0.1
0.2
0.3
0.4
0.5

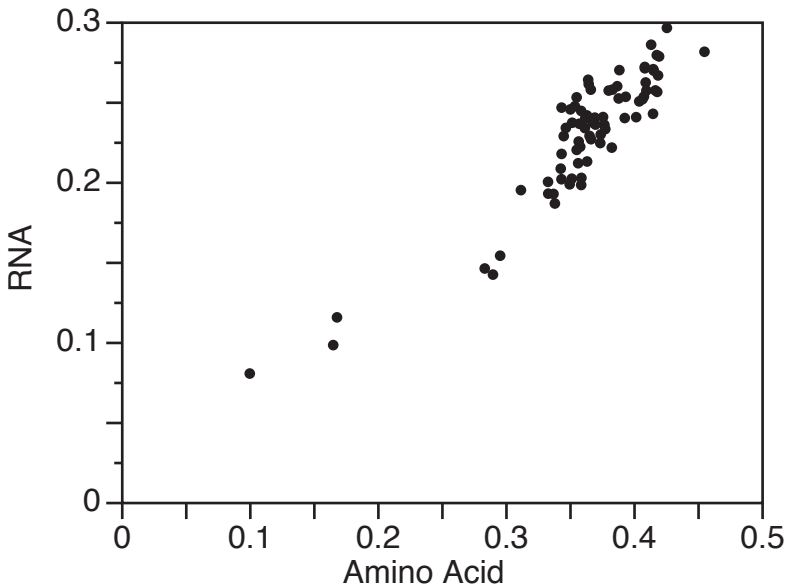
RNA
Amino Acid
0
0.1
0.2
0.3
0.4
0.5

Table S1a. Long PCR Primers, sequence and location, for *Stimulopalpus japonicus*.

Region		Primer Pair (F & R)	Sequence (5' →3')
Long PCRs			
	trnM → cox1	PSOC4 [1]	AAG CTW WTG GGY TCA TAC CYC
		STJA35 [2]	TTA ATC CCT GTA GGG ATA GC
	cox1 → cox3	C1-J-1718 [3]	GGA GGA TTT GGA AAT TGA TTA GTT CC
		C3-N-5460 [3]	TCA ACA AAG TGT CAG TAT CA
	cox3→ nad4	STJA2 [5]	TCA AGG ATT TGA ATA TTG AGA AGC
		STJA3 [5]	TCA GCC TGA GCG AAT TCA GGC TGG
	nad4 → cytB	N4-J-8944 [3]	GGA GCT TCA ACA TGA GCT TT
		cobR [4]	GCA TAA GCA AAT AAA AAA TAT CAT TC
	cytB → rrnL	STJA6 [2]	ATT GAT AAA ATC CCA TTC CAT CC
		STJA7 [2]	TTT AAT AAG GGA CGA GAA GAC CC
	rrnL → rrnS	16SB [5]	CTC CGG TTT GAA CTC AGA TCA
		SR-N-14594 [6]	AAA CTA GGA TTA GAT ACC C

[1] Primers designed from consensus sequences, for general amplification of Psocoptera

[2] Primers specifically designed for sequencing this genome

[3] Primers taken from Simon *et al*. (1994)

[4] Primers taken from Whiting (2002)

[5] Primers taken from Bybee *et al*. (2004)

[6] Primer taken from Skerratt *et al*. (2002)

Table S1b. Long PCR Primers, sequence and location, for *Amphigerontia montivaga*.

Region		Primer Pair (F & R)	Sequence (5' →3')
Long PCRs			
	cox1 → *cox3*	C1-J-1718 [3]	GGA GGA TTT GGA AAT TGA TTA GTT CC
		C3-N-5460 [3]	TCA ACA AAG TGT CAG TAT CA
	cox3→ *rrnL*	AMMO4 [2]	TGC CGA TTC AAT TTA TGG ATC GTC G
		AMMO5 [2]	TTA AAA GAC GAG AAG ACC CTA TAG
	rrnL → *rrnS*	16SB [5]	CTC CGG TTT GAA CTC AGA TCA
		SR-N-14594 [6]	AAA CTA GGA TTA GAT ACC C
	rrnS → *cox1*	AMMO8 [2]	TAG AAA GAG AAT GAC GGG CAA TAT G
		AMMO1 [2]	ATC AAC TGA TGC TCC TGT ATG TCC

[1] Primers designed from consensus sequences, for general amplification of Psocoptera

[2] Primers specifically designed for sequencing this genome

[3] Primers taken from Simon *et al*. (1994)

[4] Primers taken from Whiting (2002)

[5] Primers taken from Bybee *et al*. (2004)

[6] Primer taken from Skerratt *et al*. (2002)

Table S1c. Long PCR Primers, sequence and location, for *Lachesilla anna*.

Region		Primer Pair (F & R)	Sequence (5' →3')
Long PCRs			
	cox2 → *nad4*	FLeu [4]	TCT AAT ATG GCA GAT TAG TGC
		LAAN1 [5]	TTG TTT AAA AGA GTA GGT TCC TCC
	nad4 → *cytB*	N4-J-8944 [3]	GGA GCT TCA ACA TGA GCT TT
		cobR [4]	GCA TAA GCA AAT AAA AAA TAT CAT TC
	cytB → *rrnL*	LAAN4 [2]	TTG ATA AAG CCT CTT TTC ATC CC
		LAAN5 [2]	TTA AAA GAC GAG AAG ACC CTA TAG
	rrnL → *rrnS*	16SB [5]	CTC CGG TTT GAA CTC AGA TCA
		SR-N-14594 [6]	AAA CTA GGA TTA GAT ACC C
	rrnS → *cox2*	LAAN8 [2]	AGA GAA TGA CGG GCA ATA TGT GC
		LAAN11 [2]	ACA AAA TAC GGA GGG AAG GTA GGG C

[1] Primers designed from consensus sequences, for general amplification of Psocoptera

[2] Primers specifically designed for sequencing this genome

[3] Primers taken from Simon *et al*. (1994)

[4] Primers taken from Whiting (2002)

[5] Primers taken from Bybee *et al*. (2004)

[6] Primer taken from Skerratt *et al*. (2002)

Table S1d. Long PCR Primers, sequence and location, for *Archipsocus nomas*.

Region		Primer Pair (F & R)	Sequence (5' →3')
Long PCRs			
	trnM → cox1	ARNO7 [2]	ACG TTT TTT TCA ATT TTA CCC CGG
		RLys [4]	GAG ACC AGT ACT TGC TTT CAG TCA TC
	cox2 → nad4	ARNO11 [2]	TGC CCT TAC TGT CAA AAC TAT TGG TC
		ARNO19 [2]	AAC CTA AAG GGT TGG AAG AAC CTG
	nad4 → rrnL	N4-J-8944 [3]	GGA GCT TCA ACA TGA GCT TT
		ARNO3 [4]	TTT ATG GCG AAT TTA ATT GGG GTG
	rrnL → rrnS	16SB [5]	CTC CGG TTT GAA CTC AGA TCA
		SR-N-14594 [6]	AAA CTA GGA TTA GAT ACC C
	rrnS → trnM	ARNO4 [2]	ATA TTG CCA GTA AGA TAA TCG TGG
		TM-N-193 [3]	TGG GGT ATG AAC CCA GTA GC

[1] Primers designed from consensus sequences, for general amplification of Psocoptera

[2] Primers specifically designed for sequencing this genome

[3] Primers taken from Simon *et al*. (1994)

[4] Primers taken from Whiting (2002)

[5] Primers taken from Bybee *et al*. (2004)

[6] Primer taken from Skerratt *et al*. (2002)

Table S1e. Long PCR Primers, sequence and location, for *Speleketor irwini*.

Region		Primer Pair (F & R)	Sequence (5' →3')
Long PCRs			
	trnM → cox1	TM-J-206 [3]	TGG GGT ATG AAC CCA GTA GC
		SPIR1 [2]	AAG GAG GAT AGA CTG TTC ATC CTG
	cox1 → cox3	C1-J-1718 [3]	GGA GGA TTT GGA AAT TGA TTA GTT CC
		C3-N-5460 [3]	TCA ACA AAG TGT CAG TAT CA
	cox3→ rrnL	SPIR4 [2]	ACT ATT ACA TGA GCT CAC CAT GCA C
		SPIR5 [2]	TTT ACA TGG AAA GGG TAT TGA AGG
	rrnL → rrnS	16SB [5]	CTC CGG TTT GAA CTC AGA TCA
		SR-N-14594 [6]	AAA CTA GGA TTA GAT ACC C
	rrnS → trnM	SPIR6 [2]	TAT AGT CTG CAC CTT GAC CTG AC
		TM-N-193 [3]	TGG GGT ATG AAC CCA GTA GC

[1] Primers designed from consensus sequences, for general amplification of Psocoptera

[2] Primers specifically designed for sequencing this genome

[3] Primers taken from Simon *et al*. (1994)

[4] Primers taken from Whiting (2002)

[5] Primers taken from Bybee *et al*. (2004)

[6] Primer taken from Skerratt *et al*. (2002)

Table S1f. Long PCR Primers, sequence and location, for *Echmepteryx hageni* and *Trogium pulsatorium*.

Region		Primer Pair (F & R)	Sequence (5' →3')
Long PCRs			
	cox3→ nad4	PSOC1 [1]	TTG AAG CNG CWG CHT GRT AYT GAC
		PSOC2 [1]	AAR GCT CAT GTK GAR GCW CC

[1] Primers designed from consensus sequences, for general amplification of Psocoptera